Flow Pattern Transition Maps for Microgravity Two-Phase Flows

Subash S. Jayawardena and Vemuri Balakotaiah
Dept. of Chemical Engineering

Larry C. Witte
Dept. of Mechanical Engineering

University of Houston, Houston, TX 77204

Two-phase gas-liquid (and vapor-liquid) flows occur in a variety of process equipment such as petroleum production facilities, condensers and reboilers, power systems and core cooling of nuclear power plants during emergency operation. In addition to these normal gravity applications, two-phase flows also occur in many space operations such as active thermal control systems, power cycles, propulsion devices, and storage and transfer of cryogenic fluids.

For conditions of technological interest, there are a few major types of flow regimes observed for gas-liquid flows in pipes. Characteristics of these flow patterns and the conditions under which those flow patterns exist depends on the orientation of the pipe with respect to gravity. At low gas flow rates, a bubble flow pattern in which small gas bubbles are uniformly distributed in the liquid is obtained. Increasing the gas flow rate leads to slug flow. This flow pattern is characterized by large bullet shaped gas bubbles separated by liquid slugs. At even higher gas flow rates, a highly agitated churn flow is observed. Increasing the gas flow rate further leads to the annular flow regime in which the liquid moves along the pipe wall in a thin, wavy film and the gas flows in the core region.

The above description applies only to two-phase flows in vertical pipes. In horizontal pipes, churn flow does not exist. At low gas flow rates, smooth and wavy stratified flows exist in such pipes.

In the absence of gravity, there exist only three major flow patterns: bubble, slug, and annular (Figure 1). In microgravity, annular flows are obtained for a wide range of gas and liquid flow rates. Bubble and annular flow are the preferred flow pattern for the operation of two-phase systems in space. Slug flow is avoided, because vibrations caused by slugs result in unwanted accelerations. Therefore, it is important to be able to accurately predict the flow pattern which exists under given operating conditions of a two-phase flow system.

Ever since the early work of Baker (1958), there have been attempts to predict the transitions between flow patterns for two-phase flows in pipes. Because of the large number of dimensionless groups (seven to nine) describing the phe-

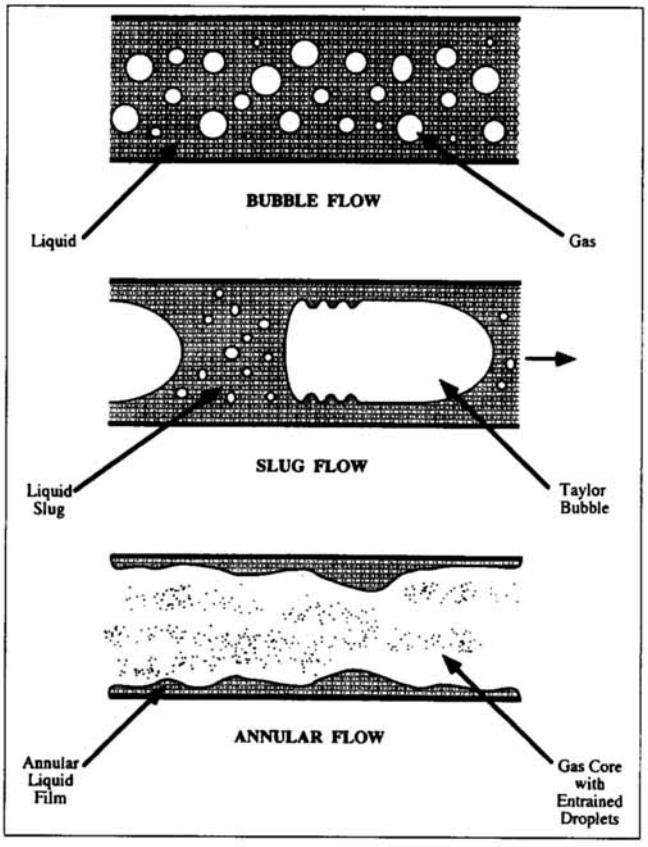

Figure 1. Flow patterns observed in microgravity two-phase flows (Bousman, 1994).

Correspondence concerning this article should be addressed to V. Balakotaiah.

nomenon, it has not been possible to correlate the experimental data and present the transition maps in a more general (dimensionless) form, independent of the specific system. Most flow pattern maps in the literature are presented using the gas and liquid velocities and are applicable only to specific systems. An example of this is the map by Dukler and Taitel (1986). One exception is the work of Zhao and Rezkallah (1993), which uses the Weber number (defined as $We_{GS} = \rho_G U_{GS}^2 D/\sigma$).

Approach

For two-phase flows in zero gravity, the number of dimensionless groups is reduced by two because of the inherent symmetry present (no preferred orientation for the pipe) and the absence of gravity. A dimensional analysis shows that for smooth pipes, there are five dimensionless groups that are relevant: the gas and liquid Reynolds numbers ($Re_{GS} = \rho_G U_{GS} D/\mu_G$ and $Re_{LS} = \rho_G U_{LS} D/\mu_L$); the Weber number ($We_{LS} = \rho_L U_{LS}^2 D/\sigma$); and ratios of gas to liquid densities and viscosities. (In place of the Weber number, we could also use the Capillary number $Ca = \mu_L U_{LS}/\sigma$). Here, U_{LS} is the superficial velocity of the liquid based on a single-phase flow and U_{GS} is the superficial gas velocity. Intuitively, we expect the flow pattern transition boundary to be a weak function of the last two ratios, as long as these ratios remain much smaller than unity. (By this statement, we mean that terms like $1 \pm (\rho_G/\rho_L)$ can be replaced by unity.) This assumption reduces the number of most relevant dimensionless groups to three. In addition, if the flow conditions and pipe diameter are such that the capillary effects are not dominant, then it is possible to correlate the flow pattern maps in terms of two dimensionless groups by combining the Weber (or the Capillary number) with the Reynolds number.

We have developed a flow pattern transition map for microgravity two-phase flows using two dimensionless parameters. Our results suggest that flow pattern transition in microgravity can be predicted using the maps shown in Figures 2 and 3. These were developed using experimental data collected by many researchers (see Table 1) using different working fluids and tube sizes. These maps suggest the importance of a dimensionless group called Suratman number ($Su = Re_{LS}^2/We_{LS} = \sigma D \rho_L/\mu_L^2$) in determining the transitions between the flow patterns. (In the literature, the reciprocal of the square root of Su, called the Ohnesorge number, is also used. However, we prefer to use the Suratman number for the reasons explained below.) The Suratman number is the ratio of Reynolds number (Re_L) to the Capillary number. It may be interpreted as the ratio of the product of surface tension and inertia forces to the square of the viscous forces. It is the natural parameter that arises when the characteristic velocity used in the definition of the liquid Reynolds number (Re_{LS}) is replaced by the capillary velocity ($U_c = \sigma/\mu_L$).

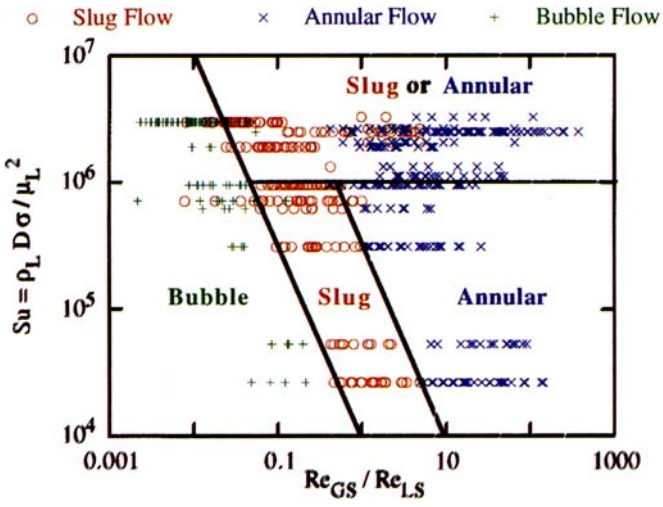

Figure 2. Flow pattern map for microgravity two-phase flows.

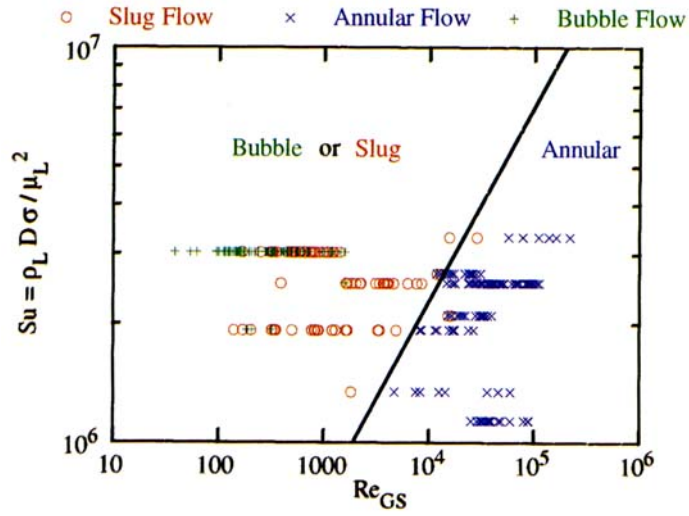

Figure 3. Flow pattern map to identify annular flows in microgravity (when $Su > 10^6$).

Table 1 summarizes different sources of experimental data used in developing the maps shown in Figures 2 and 3. Since the identification of the flow pattern near a transition boundary is a highly subjective matter, we have not used flow patterns which were identified as bubble-slug or slug-annular in obtaining the proposed flow pattern map. When those experimental data points are plotted on the proposed maps, they were located around the transition boundaries. It will be interesting to check the original flow visualization data to see whether two-phase flows of such transitional points predominantly indicate the features corresponding to the flow pattern suggested by the proposed maps.

Bubble-slug transition

According to the proposed flow pattern map, bubble-slug flow pattern transition for the range of Suratman numbers studied ($10^4 < Su < 10^7$) occurs at a particular value of the ratio (Re_{GS}/Re_{LS}). This transitional value $(Re_{GS}/Re_{LS})_t$, increases with decreasing Suratman number according to the relationship

$$\left(\frac{Re_{GS}}{Re_{LS}}\right)_t = K_1 Su^{-2/3} \qquad (1)$$

where the numerical value of the constant K_1 is found to be

Table 1. Sources of Microgravity Flow Pattern Information

Source	Fluid		Dia.	No. of Observations		
	Liquid	Vapor	(m)	Bubble	Slug	Annular
Janicot (1988)	water	air	0.0127	6	16	12
Bousman (1994)	water	air	0.0127	7	30	33
	water-glycerin	air	0.0127	4	22	31
	water-zonyl	air	0.0127	4	16	31
	water	air	0.0254	3	30	14
	water-glycerin	air	0.0254	5	11	15
	water-zonyl	air	0.0254	4	9	8
Colin (1990)	water	air	0.0400	83	48	n/a
Zhao and Rezkallah (1993)	water	air	0.009525	6	46	43
Huckerby and Rezkallah (1992)	water	air	0.009525	8	25	n/a
Crowley and Sam (1991)	R11	R11	0.00634	n/a	2	8
Reinarts (1993)	R12	R12	0.0127	1	21	62
	R12	R12	0.0047	n/a	n/a	22
Hill and Best (1991)	R12	R12	0.0111	n/a	16	3
	R12	R12	0.0087	n/a	16	3
Chen et al. (1988)	R114	R114	0.0158	n/a	2	6

464.16. We note that this transition boundary may also be expressed as

$$(Re_{GS})_t = K_1 Re_{LS}^{1/3} Ca^{2/3} \tag{2}$$

Slug-annular transition

Unlike the bubble-slug transition, the slug annular transition is not given by a single straight line. For $Su < 10^6$, the transition line has the same slope as the bubble-slug transition. However, for $Su > 10^6$, the gas Reynolds number at the transition is proportional to the square of the Suratman number. Thus, the slug-annular transition is found to be

$$(Re_{GS}/Re_{LS})_t = K_2 Su^{-2/3} \quad \text{for} \quad Su < 10^6 \tag{3a}$$

$$(Re_{GS})_t = K_3 Su^2 \quad \text{for} \quad Su > 10^6, \tag{3b}$$

where K_2 and K_3 are numerical constants ($K_2 = 4{,}641.6$, $K_3 = 2 \times 10^{-9}$).

Since the Suratman number is determined by the tube diameter and physical properties of the fluid, we can use the proposed maps to identify the flow pattern for a given two-phase system with known liquid and vapor flow rates.

Discussion

Table 2 compares the number of prior observations which agree with the predicted flow pattern maps of Figures 2 and 3. It shows the number of data points of each flow pattern falling into regions of the maps identified as bubble, slug, or annular. Off-diagonal elements indicate where the predicted flow pattern does not agree with the experimentally observed flow pattern. It is clear that the proposed map has never predicted a bubble flow pattern for conditions which actually result in annular flow pattern and vice versa. Inaccuracies arise only when predicting between bubble and slug, or between slug and annular flow patterns. Table 2 is divided into two sections depending on the Suratman number. We estimated the accuracy of a prediction as the ratio of the number of correct predictions to the total number of data points around the transition under consideration. This procedure suggests that for $Su < 10^6$, we can predict the flow pattern map with about 93% overall accuracy. Specifically, the accuracy of the prediction between bubble and slug regimes is about 94% and the accuracy of the prediction between slug and annular regimes is about 95%. For $Su > 10^6$, the overall accuracy is about 91%. Specifically, the accuracy of the prediction between bubble and slug regimes is about 87% and the accuracy of the prediction between slug and annular regimes is about 97%.

Though it was attempted to propose a single map to predict bubble, slug, and annular flow regimes, it was only possible to propose two maps with different coordinates. If $Su < 10^6$, the procedure is straightforward. Otherwise, first use the Eq. 1 to decide whether the flow regime is bubble or not. If the flow pattern is not bubble flow, then use Eq. 3b to determine whether it is slug or annular.

The discrepancies between observed and predicted flow patterns (as summarized in Table 2) may be due to the difficulty and the subjective nature of identifying flow pattern (specially between bubble and slug) under conditions around

Table 2. Accuracy of Predictions Using Proposed Maps

Observed ↓	Predicted					
	$Su < 10^6$			$Su > 10^6$		
	Bubble	Slug	Annular	Bubble	Slug	Annular
Bubble	37	1	0	71	15	0
Slug	8	110	10	10	92	4
Annular	0	2	129	0	2	142

the transition boundary. This is the same reason why the data points that were identified as bubble-slug or slug-annular were not used in this work. Also, it is unknown whether observed flow pattern in such tests would have changed if the flow development length or duration was longer.

The proposed maps suggest a dramatic change in the behavior at a Suratman number around 10^6, causing changes in the slug-annular transition. It is not just a change in the slope of the transition boundary line, but also a change of the horizontal coordinate from (Re_{GS}/Re_{LS}) to Re_{GS}. The reasons for such a dramatic change needs to be explored in detail. Since the asymptotic behavior of these maps should agree around the Suratman number of 10^6, we do not expect a sudden transition of the mechanism. The detailed behavior for conditions when the Suratman number is close to 10^6 is still not clear. The maps shown in Figures 2 and 3 may not be valid for very low values of the Suratman number. The experimental data available is limited to a range above about 10^4. More experiments need to be conducted in the low Suratman number region to assess the importance of capillary effects.

The flow pattern transition from annular to slug flow is affected by the growth rates of the disturbances on the deformable gas-liquid (vapor-liquid) interface. Therefore, detailed information on the liquid film behavior should be obtained to understand the basic reason for this change in flow pattern transition mechanism. We are not aware of any study, in which detailed measurements of annular two-phase flow are made at a Suratman number greater than 10^6. An example for such a system is a large diameter two-phase system with a refrigerant as the working fluid.

The flow pattern maps proposed here can be used to obtain flow pattern transition boundaries of dimensional flow pattern maps suggested by Dukler et al. (1988). Instead of using a critical void fraction to estimate the position of the transition boundary, we will obtain that information using the Suratman number and fluid properties of the two-phase system. Colin et al. (1996) looked at the void-fraction based model of Dukler et al. (1988) for microgravity bubble-slug transition and suggested the existence of a critical Suratman number of 1.6×10^6. They observed different values for the critical void fraction above and below that number.

The approach taken here may be applied to develop normal gravity flow pattern maps. As stated in the introduction, flow pattern transition in normal gravity is complicated because of the additional parameters (magnitude and direction of the gravity vector). But, at the limit of high Froude numbers, the maps developed here might also be valid for normal gravity two-phase flows. Two-phase flows in vertical pipes resemble microgravity conditions because of the symmetry. Thus, the proposed maps may give a starting point for two-phase flow pattern maps in vertical pipes at high Froude numbers. Since a two-dimensional map limits the number of independent dimensionless groups to two, different flow pattern maps might have to be constructed for different Froude numbers ($Fr = U^2/gD$) or Bond numbers ($Bo = \sigma/\rho gD^2$).

Conclusions

For microgravity two-phase flows, a novel flow pattern map based on dimensionless parameters is proposed. This indicated the dependence of bubble-slug and slug-annular transitions on the Suratman number of the system. The bubble-slug transition occurs at a transitional value of the gas to liquid Reynolds number ratio, which decreases with increasing Suratman number. The slug-annular transition occurs at a different transitional value of the gas to liquid Reynolds number ratio, which decreases with increasing Suratman number for low Suratman number systems. For high Suratman number systems, the slug-annular transition occurs at a transitional value of the gas Reynolds number, which increases with increasing Suratman number. The empirically determined flow pattern transition boundaries are straight lines (on the log-log scale) with slopes equal to $-2/3$ or 2, and the significance of these numbers is yet to be understood. These flow pattern maps also provide a starting point to create dimensionless flow pattern maps for high Froude number normal gravity two-phase flows.

Acknowledgments

This work is supported by grants from the NASA-Lewis Research Center (NAG3-1840) and the UH-JSC aerospace post-doctoral fellowship program.

Literature Cited

Baker, O., "Multiphase Flow in Pipe Lines," *Oil and Gas J.*, 156 (1958).

Bousman, W. S., "Studies of Two-Phase Gas-Liquid Flow in Microgravity," PhD Diss., Univ. of Houston (1994).

Chen, I., R. Downing, R. Parish, and E. Keshock, "A Reduced Gravity Flight Experiment: Observed Flow Regimes and Pressure Drops of Vapor and Liquid Flow in Adiabatic Piping," *Proc. AIChE Heat Transfer Conf.*, Houston (1988).

Colin, C., J. Fabre, and J. McQuillen, "Bubble and Slug Flow at Microgravity Conditions," *Chem. Eng. Comm.*, 141 (1996).

Colin, C., "Ecoulements Disphasiques a Bulles et a Poches en Micropesanteur," MS Thesis, Institut de Mecaniques des Fluides de Toulouse, France (1990).

Crowley, C. J., and R. G. Sam, "Microgravity Experiments with a Simple Two-Phase Thermal System," Report No. PL-TR-91-1059, Phillips Lab. Kirtland Air Force Base, NM (1991).

Dukler, A. E., and Y. Taitel, "Flow Pattern Transitions in Gas-Liquid Flows: Measurements and Modeling," *Multiphase Sci. Technol.*, **2**, 1 (1986).

Dukler, A. E., J. A. Fabre, J. B. McQuillen, and R. Vernon, "Gas-Liquid Flow at Microgravity Conditions: Flow Patterns and Their Transitions," *Int. J. Multiphase Flow*, **14**(4), 389 (1988).

Hill, W. S., and F. R. Best, "Microgravity Two-Phase Flow Experiment and Test Results," *SAE Tech. Paper Ser. 911556*, Int. Conf. on Env. System, San Francisco, (July 15–18, 1991).

Huckerby, C. S., and K. S. Rezkallah, "Flow Pattern Observations in Two-Phase Gas Liquid Flow in a Straight Tube under Normal and Microgravity Conditions," *Proc. of Nat. Heat Transf. Conf.*, AIChE, San Diego (July, 1992).

Janicot, A. J. P., "Experimental and Theoretical Studies of Gas-Liquid Two-Phase Flow at Reduced Gravity Conditions," MS Thesis, Univ. of Houston (1988).

Reinarts, T. R., "Adiabatic Two Phase Flow Regime Data and Modeling for Zero and Reduced (Horizontal Flow) Acceleration Fields," PhD Diss., Texas A&M Univ., College Station (1993).

Zhao, L., and K. S. Rezkallah, "Gas-Liquid Flow Patterns at Microgravity Conditions," *Int. J. Multiphase Flow*, **19** (1993).

Manuscript received Nov. 5, 1996, and revision received Jan. 13, 1997.